SUPPLEMENTARY MATERIALS
Worldwide soil moisture changes driven by future hydro-climatic change scenarios

Lucile Verrot[1], Georgia Destouni[1]

[1]Department of Physical Geography & Bolin Centre for Climate Research, Stockholm University, SE-106 91 Stockholm, Sweden

Correspondence to: Lucile Verrot (lucile.verrot@natgeo.su.se)

Contents :

Figure S7. Map of model result agreement between the two radiative forcing scenarios RCP 2.6 and RCP 8.5, regarding the change in inter-annual variability of seasonal soil moisture during the dry and the wet season.

Supplementary Sections

1. Model and catchment selection

From the original 608 catchments from the Global Runoff Data Center (GRDC, 2015) database with an area over 100'000 km^2, we finally selected 81 study catchments. Regarding the CMIP5 models, there were originally 20 models providing the required *mrros, mrro* and *pr* outputs, from which a final set of 14 CMIP5 models was selected (Table S1).

The first selection step was to discard the models providing too many time series with only constant values for either *mrro* or *mrros* (none of the models was giving constant *pr* values). As a first step, the maximum number of catchments with constant value tolerated for a model was set to 40. It means that if a model was giving a constant time series for more than 40 catchments, we discarded it. Then, from the remaining models, the catchments that had a constant time series from at least one model were further discarded.

The second selection step was to discard the models yielding too many negative values for R_{eff} as calculated from *mrro* and *mrros* (see main Eq. 4). As a first step, we discarded models providing at least one negative value in their R_{eff} time series for more than 154 catchments (arbitrary first-step threshold). Furthermore, the catchments were then discarded that had at least one negative value in their R_{eff} time series from any of the remaining models. Table S2 summarizes the models and number of catchments discarded in those two selection steps, for each of the RCP 2.6 and RCP 8.5 scenarios. Finally, after all smaller nested catchments were removed, the final set of 81 study catchments (main Fig. 1) and 14 CMIP5 models (Table S1) emerged for this study.

S2. Quantification of agreement between RCP 2.6 and RCP 8.5

In order to quantify the differences between the projected changes under the climate change scenario RCP 2.6 and those under the scenario RCP 8.5, we calculated a simple indicator of agreement a [-] for each catchment:

$$a = \frac{min(|v_1|, |v_2|)}{max(|v_1|, |v_2|)} \; if \; sgn(v_1) = sgn(v_2) \quad \text{(S1-a)}$$

$$a = -\frac{min(|v_1|, |v_2|)}{max(|v_1|, |v_2|)} \; if \; sgn(v_1) \neq sgn(v_2) \quad \text{(S1-b)}$$

Where v_1 is the value of the variable (in our study, the frequency of dry/wet events, the mean seasonal soil moisture, or the inter-annual variability of the latter) under RCP 2.6 and v_2 is the value of the variable under RCP 8.5. Furthermore, *sgn(x)* is the sign function: it returns -1 if $x<0$ and 1 if $x>0$; v_1 and v_2 are always different from 0. From Eq. S1-a and S1-b, the agreement value *a* will have a negative value if the sign of v_1 and v_2 are different (represented in two shades of red in the SM Fig. S5, S6 and S7), and a positive value if they are of the same sign (represented in two shades of green in the Fig. S5, S6 and S7).

Supplementary Bibliography

FAO/IIASA/ISRIC/ISSCAS/JRC: Harmonized World Soil Database (version 1.2). FAO, Rome, Italy and IIASA, Laxenburg, Austria, 2012.

GRDC, The Global Runoff Data Centre, D - 56002 Koblenz, Germany, Federal Institute of Hydrology (BfG), retrieved in October 2015.

Landerer, F. W., and Swenson S.C.: Accuracy of scaled GRACE terrestrial water storage estimates. *Water Resources Research*, 48(4). doi:10.1029/2011WR011453, 2012

Nachtergaele, F., Van Velthuizen, H., Verelst, L., Batjes, N., Dijkshoorn, K., Van Engelen, V., Fischer, G., Jones A., Montanarella L., Petri M., and Prieler, S.: Harmonized world soil database, Food and Agriculture Organization of the United Nations, 2008.

ORNL DAAC: MODIS subsetted land products, collection 5. Oak Ridge National Laboratory Distributed Active Archive Center (ORNL DAAC), Oak Ridge, Tennessee, USA, 2011. <http://daac.ornl.gov/MODIS/modis.html> (accessed 5.10.2015).

Rawls, W.J., Brakensiek, D.L., and Saxton, K.E.; Estimation of soil water properties, Transactions of the American Society of Agricultural Engineers 25: 1316–1320, 1982.

Schneider, U., Becker, A., Finger, P., Meyer-Christoffer, A., Rudolf, B., and Ziese, M.: GPCC full data reanalysis version 6.0 at 0.5: monthly land-surface precipitation from rain-gauges built on GTS-based and historic data. doi: 10.5676/DWD_GPCC. FD_M_V6_050, 2011.

Swenson, S.C.: GRACE monthly land water mass grids NETCDF RELEASE 5.0. Ver. 5.0. PO.DAAC, CA, USA. Dataset accessed 2015-12-02 at http://dx.doi.org/10.5067/TELND-NC005, 2012.

Swenson, S., and Wahr J.: Post-processing removal of correlated errors in GRACE data. *Geophysical Research Letters*, 33(8). doi:10.1029/2005GL025285, 2006.

Verrot, L., and Destouni, G.: Data-model comparison of variability in long-term time series of large-scale soil moisture, In review, 2016.

Supplementary Tables

Table S1. Final selected set of 14 CMIP5 models for this study.

Model Name	Institution
BNU-ESM	College of Global Change and Earth System Science, Beijing Normal University
CCSM4	National Center for Atmospheric Research
CESM1-CAM5	Community Earth System Model, Community Atmosphere Model
CSIRO-Mk3.6.0	Commonwealth Scientific and Industrial Research Organization in collaboration with Queensland Climate Change Centre of Excellence
FGOALS-g2	Flexible Global Ocean-Atmosphere-Land System Model
FIO-ESM	The First Institute of Oceanography, SOA, China
GISS-E2-H GISS-E2-R	NASA Goddard Institute for Space Studies
IPSL-CM5A-MR	Institut Pierre-Simon Laplace
MPI-ESM-MR MPI-ESM-LR	Max-Planck-Institut für Meteorologie (Max Planck Institute for Meteorology)
MRI-CGCM3	Meteorological Research Institute
NorESM1-MNorESM1-ME	Norwegian Climate Centre

Table S2. Models and number of catchments discarded in the two model-catchment selection steps described in section S1.

	Scenario RCP 2.6	Scenario 8.5
Step 1: models giving >40 constant time series	IPSL-CM5A-LR MIROC-ESM	IPSL-CM5A-LR MIROC-ESM
Number of catchments with constant time series	26	27
Step 2: models giving >154 time series with at least one negative R_{eff} value	BCC-CSM1.1 BCC-CSM1.1(m) CNRM-CM5 MIROC-ESM MIROC5	BCC-CSM1.1 BCC-CSM1.1(m) CNRM-CM5 MIROC-ESM MIROC5
Number of catchments with constant time series	192	203

Table S3. Soil hydraulic parameters for different soil texture types after Rawls et al. (1982).

Soil texture	K_s (m/s)	θ_{ir} (-)	θ_s (-)	β (-)
Sand	5.83×10^{-4}	0.02	0.44	0.17
Loamy sand	1.70×10^{-4}	0.04	0.44	0.15
Sandy loam	7.19×10^{-5}	0.04	0.45	0.12
Loam	3.67×10^{-5}	0.03	0.46	0.09
Silt loam	1.89×10^{-5}	0.02	0.50	0.09
Sandy clay loam	1.19×10^{-5}	0.07	0.40	0.11
Clay loam	6.39×10^{-6}	0.08	0.46	0.09
Silty clay loam	4.17×10^{-6}	0.04	0.47	0.07
Sandy clay	3.34×10^{-6}	0.11	0.43	0.08
Silty clay	2.50×10^{-6}	0.06	0.48	0.06
Clay	1.67×10^{-6}	0.09	0.48	0.07

Supplementary figures

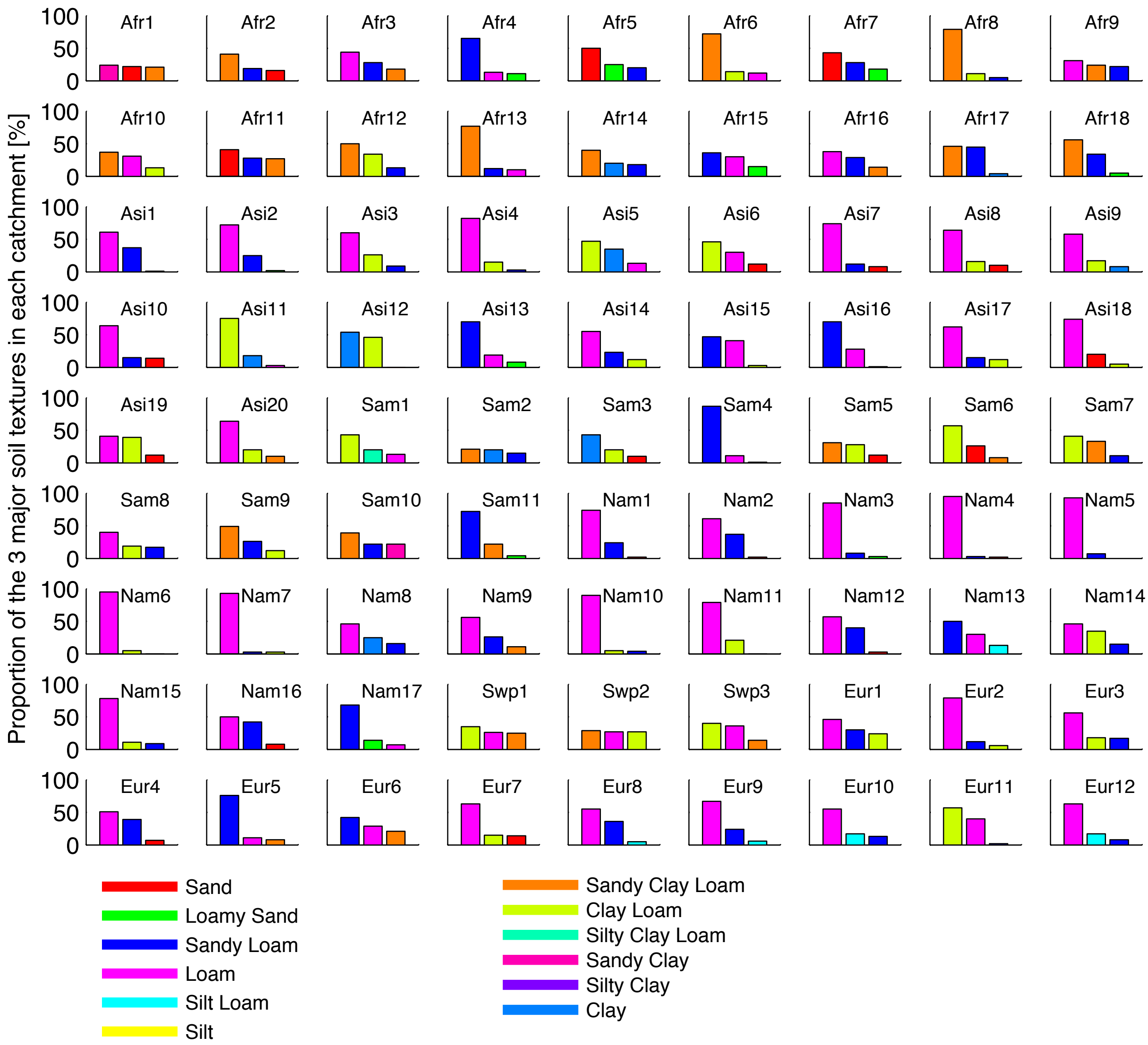

Figure S1. Proportion of the three major USDA soil textures prevailing in the catchments, as given from (Nachtergaele et al., 2008). For the calculations of θ_{uz} (main Eq. 3), only the dominant soil texture in each catchment (left bar in each bar plot) was used. The second and third most important soil textures in each catchment are represented by the middle and right bar in each subplot, respectively.

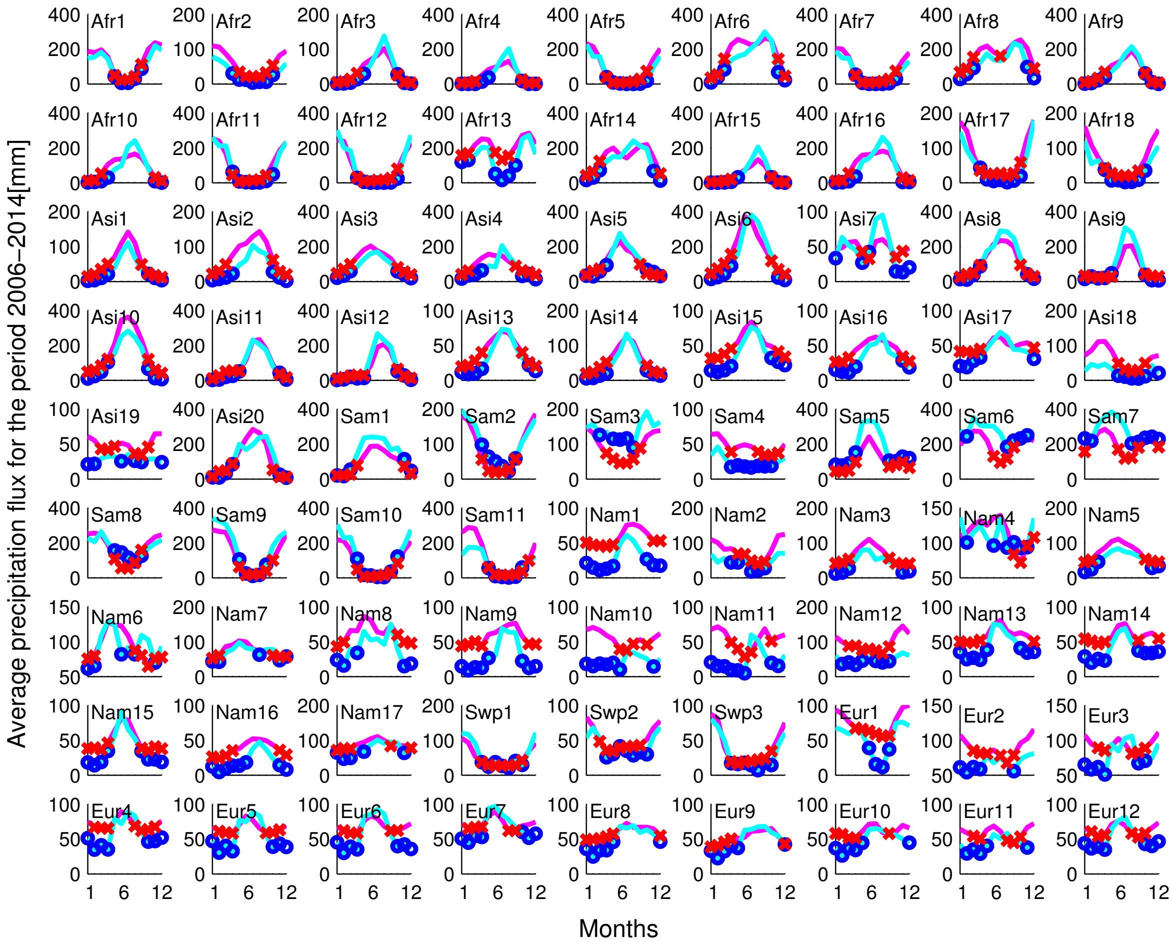
Average precipitation flux for the period 2006−2014[mm]
Afr1 Afr2 Afr3 Afr4 Afr5 Afr6 Afr7 Afr8 Afr9
Afr10 Afr11 Afr12 Afr13 Afr14 Afr15 Afr16 Afr17 Afr18
Asi1 Asi2 Asi3 Asi4 Asi5 Asi6 Asi7 Asi8 Asi9
Asi10 Asi11 Asi12 Asi13 Asi14 Asi15 Asi16 Asi17 Asi18
Asi19 Asi20 Sam1 Sam2 Sam3 Sam4 Sam5 Sam6 Sam7
Sam8 Sam9 Sam10 Sam11 Nam1 Nam2 Nam3 Nam4 Nam5
Nam6 Nam7 Nam8 Nam9 Nam10 Nam11 Nam12 Nam13 Nam14
Nam15 Nam16 Nam17 Swp1 Swp2 Swp3 Eur1 Eur2 Eur3
Eur4 Eur5 Eur6 Eur7 Eur8 Eur9 Eur10 Eur11 Eur12
1 6 12
Months

(a)

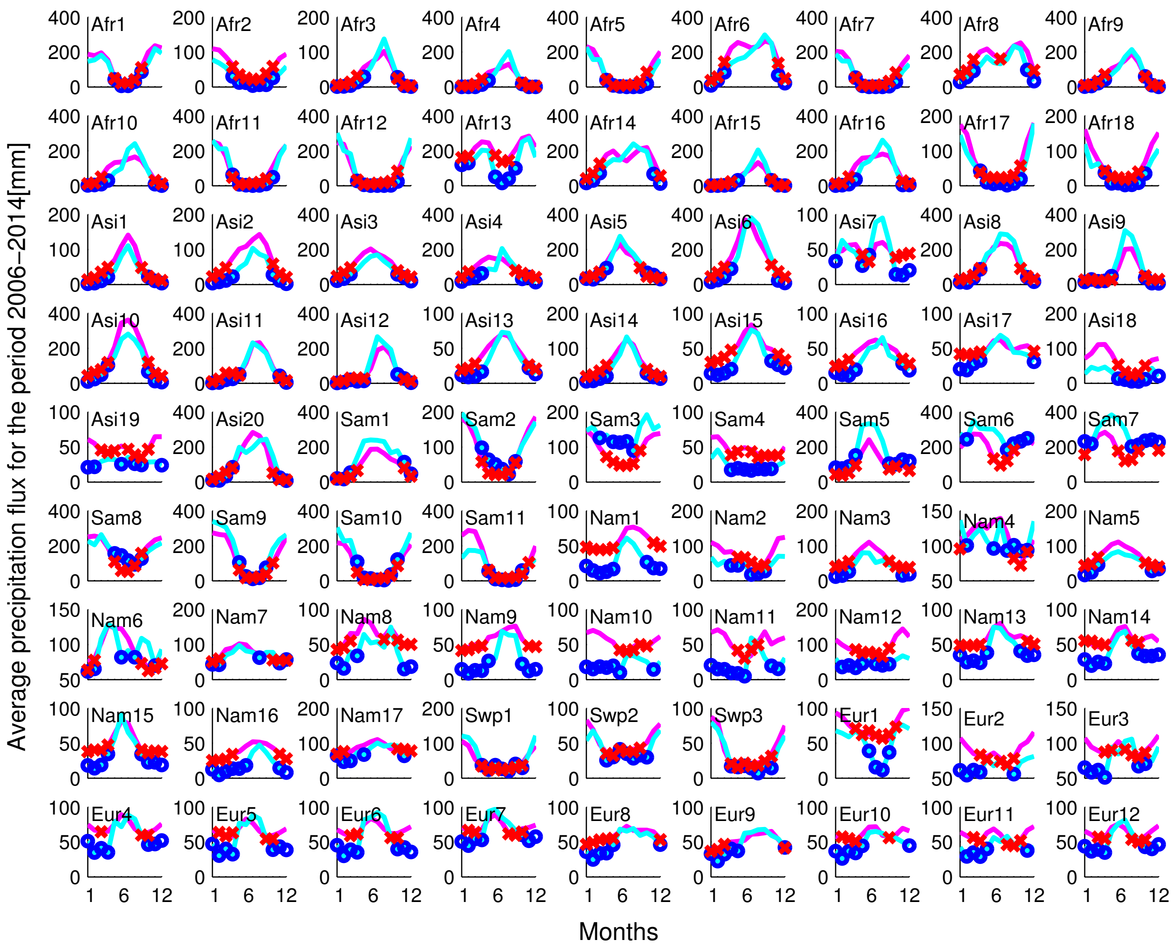
Average precipitation flux for the period 2006−2014[mm]
Afr1 Afr2 Afr3 Afr4 Afr5 Afr6 Afr7 Afr8 Afr9
Afr10 Afr11 Afr12 Afr13 Afr14 Afr15 Afr16 Afr17 Afr18
Asi1 Asi2 Asi3 Asi4 Asi5 Asi6 Asi7 Asi8 Asi9
Asi10 Asi11 Asi12 Asi13 Asi14 Asi15 Asi16 Asi17 Asi18
Asi19 Asi20 Sam1 Sam2 Sam3 Sam4 Sam5 Sam6 Sam7
Sam8 Sam9 Sam10 Sam11 Nam1 Nam2 Nam3 Nam4 Nam5
Nam6 Nam7 Nam8 Nam9 Nam10 Nam11 Nam12 Nam13 Nam14
Nam15 Nam16 Nam17 Swp1 Swp2 Swp3 Eur1 Eur2 Eur3
Eur4 Eur5 Eur6 Eur7 Eur8 Eur9 Eur10 Eur11 Eur12
1 6 12
Months

(b)


CMIP5
GPCC

Figure S2. Mean monthly precipitation (in mm) from the GPCC dataset (Schneider et al. 2011) (light blue line) and from the CMIP5 ensemble mean of the 14 models in Table S1 (pink line). Results are shown for each catchment and the period 2006-2014, and for both radiative forcing scenarios RCP 2.6 in panel (a) and RCP 8.5 in panel (b). The month numbering is: January as month 1 through to December as month 12. The markers on the lines represent the dry season months according to the season definition given in the main section 2.4. The blue markers are the dry season months determined from the GPCC dataset and the red markers are the dry season months determined from the CMIP5 model ensemble mean.

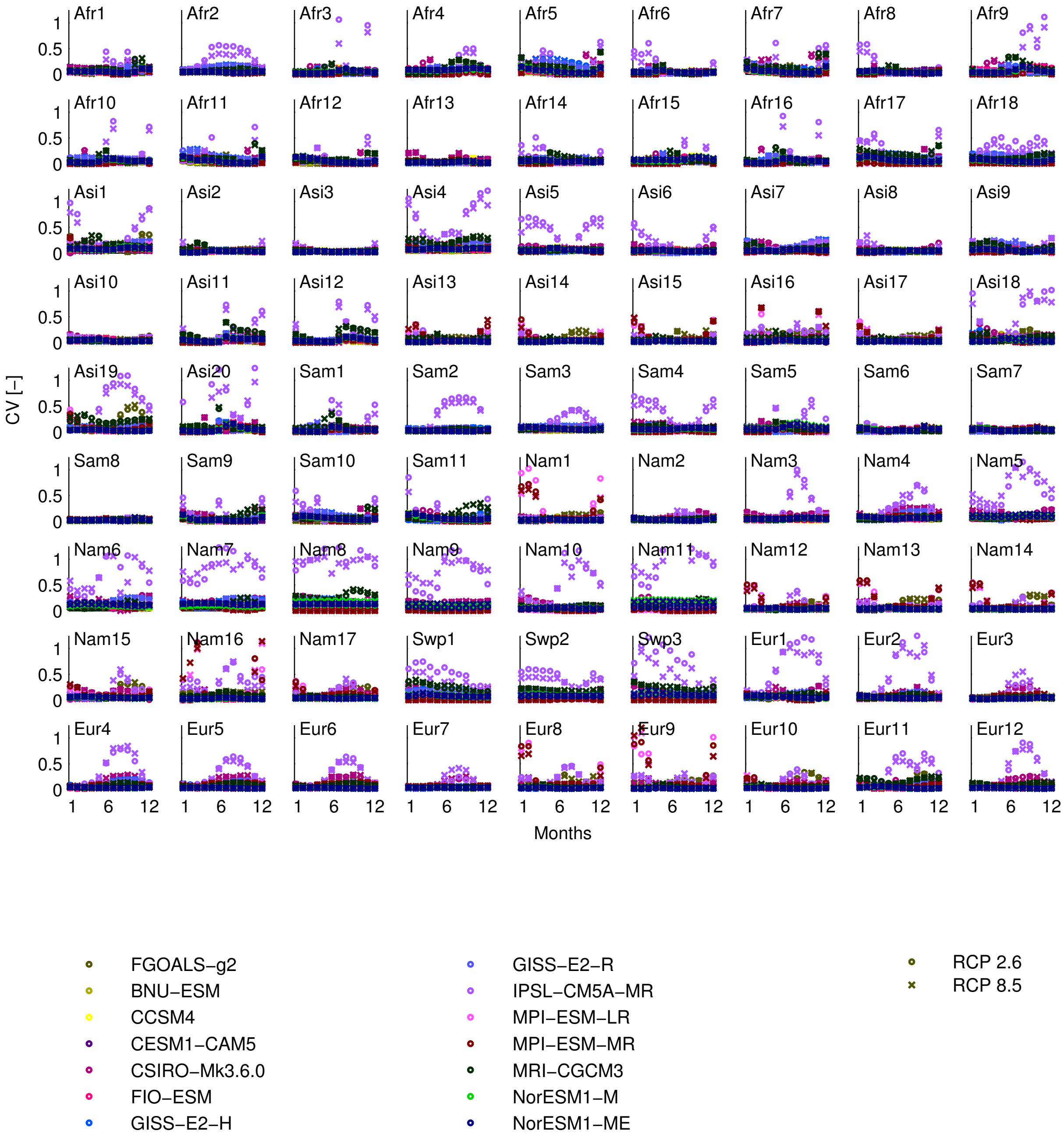

Figure S3. Coefficient of variation (standard deviation divided by the long-term mean value) of monthly average unsaturated soil water content among the years in study period 2006-2099. Results are shown for each of the 14 CMIP5 models (Table S1), both climate scenarios ('o' marker for RCP 2.6 and 'x' marker for RCP 8.5). The months numbering is: January as month 1 through to December as month 12.

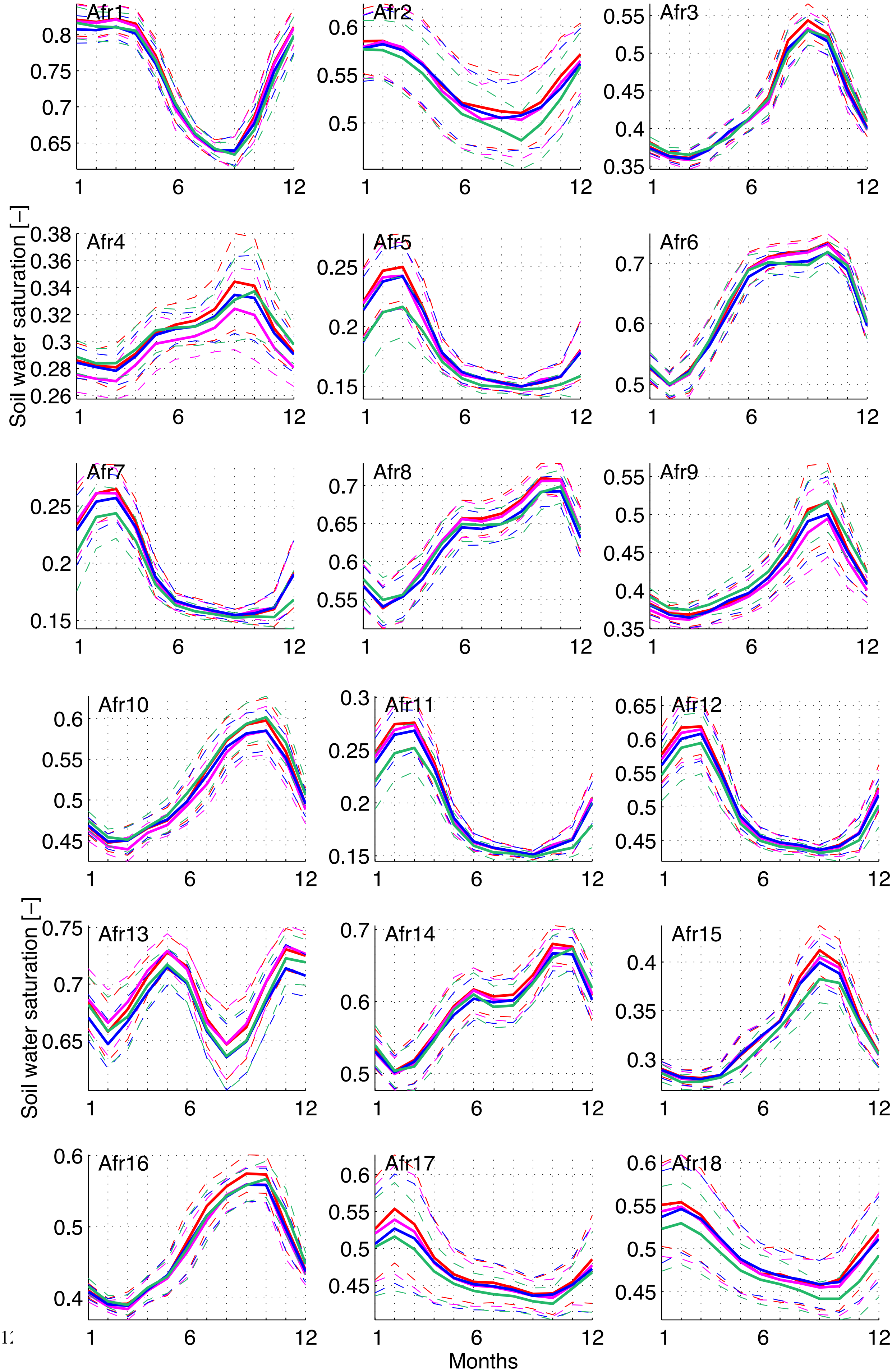

Afr1
Afr2
Afr3
Afr4
Afr5
Afr6
Afr7
Afr8
Afr9
Afr10
Afr11
Afr12
Afr13
Afr14
Afr15
Afr16
Afr17
Afr18
Soil water saturation [–]
Soil water saturation [–]
Months

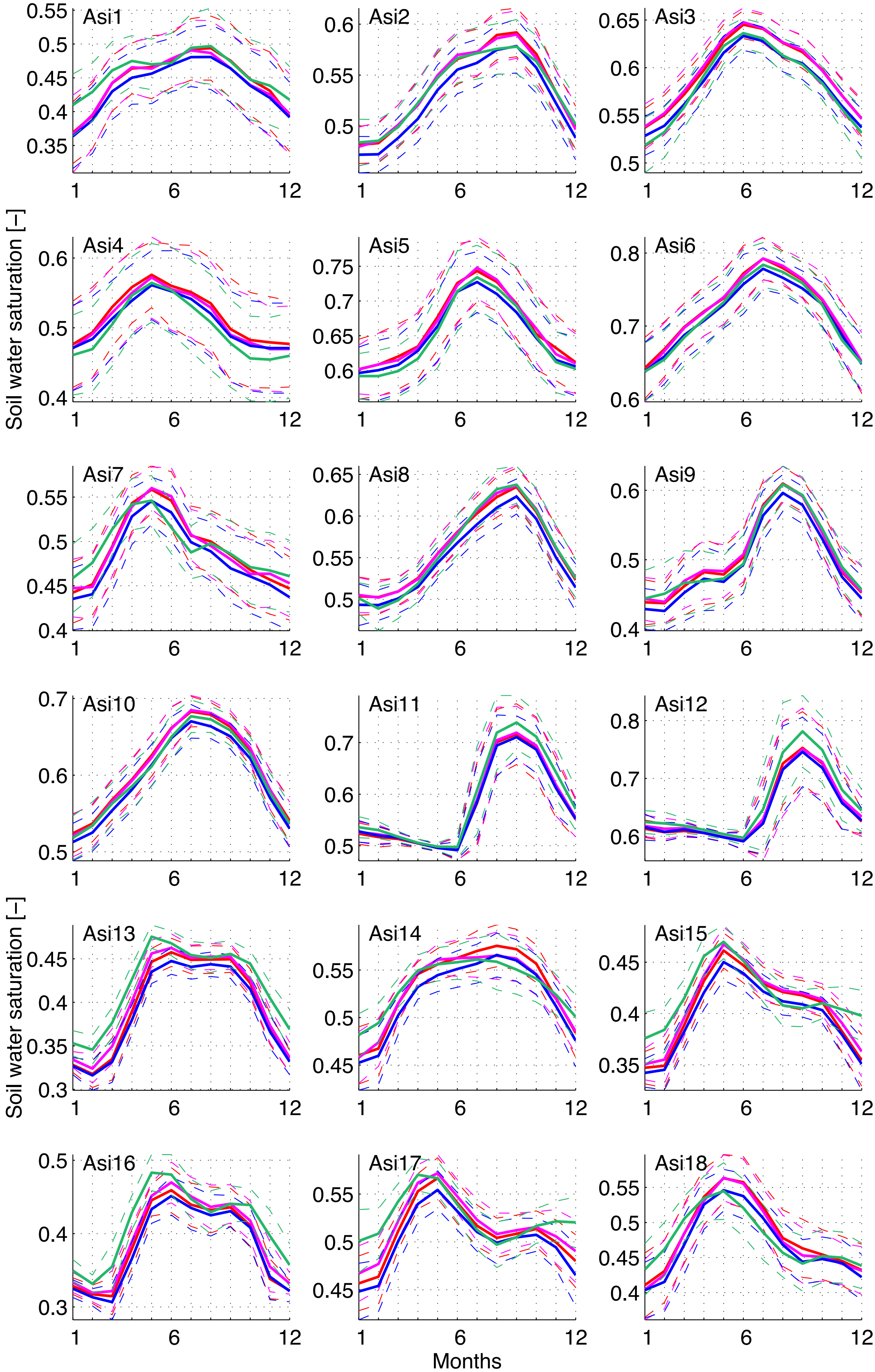

Asi1
Asi2
Asi3
Asi4
Asi5
Asi6
Asi7
Asi8
Asi9
Asi10
Asi11
Asi12
Asi13
Asi14
Asi15
Asi16
Asi17
Asi18
Soil water saturation [–]
Soil water saturation [–]
Months

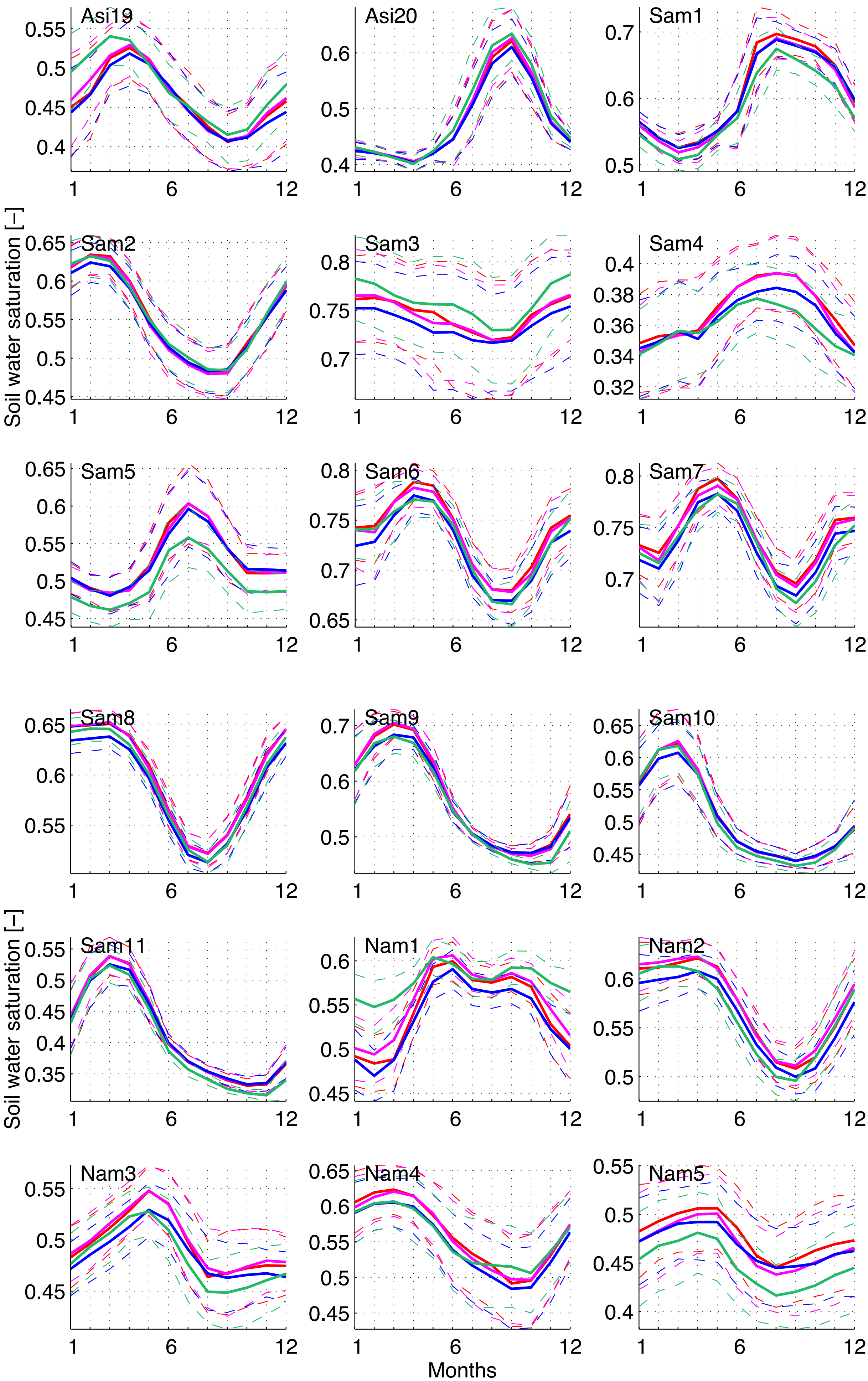
Asi19
Asi20
Sam1
Sam2
Sam3
Sam4
Sam5
Sam6
Sam7
Sam8
Sam9
Sam10
Sam11
Nam1
Nam2
Nam3
Nam4
Nam5
Soil water saturation [–]
Soil water saturation [–]
1
6
12
Months

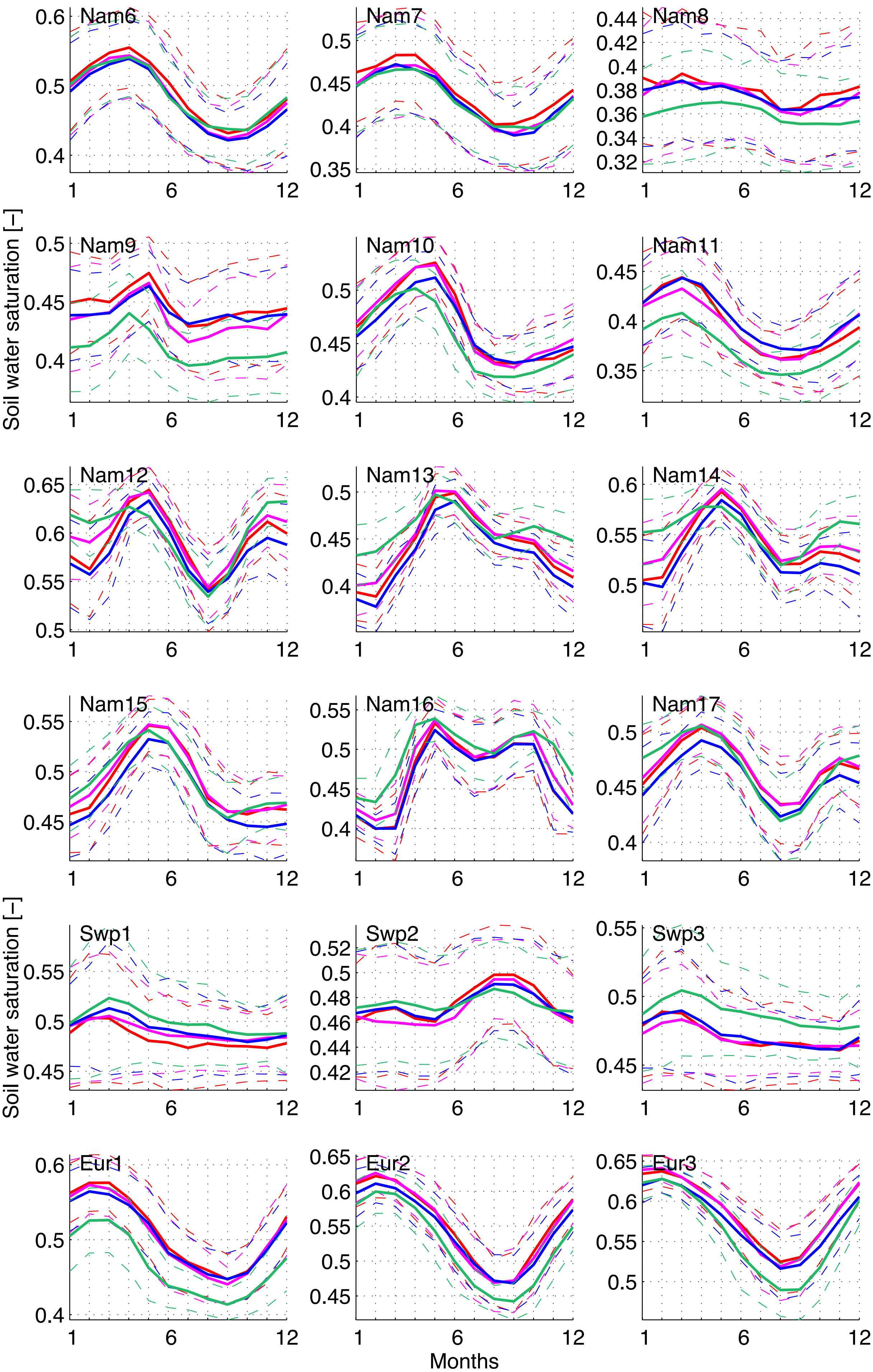
Nam6
Nam7
Nam8
Nam9
Nam10
Nam11
Nam12
Nam13
Nam14
Nam15
Nam16
Nam17
Swp1
Swp2
Swp3
Eur1
Eur2
Eur3
Soil water saturation [-]
Soil water saturation [-]
Months

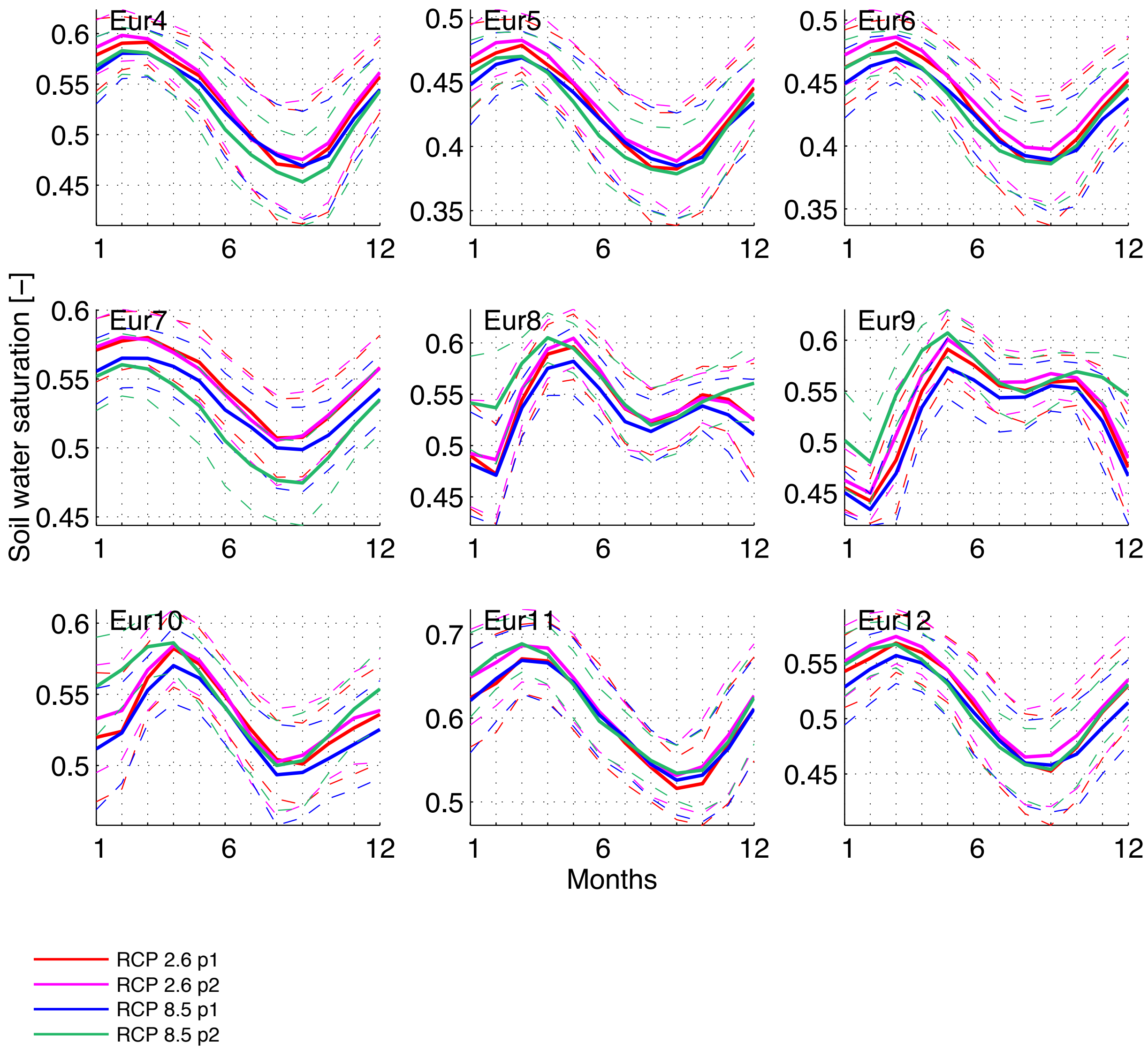

Figure S4. Mean monthly relative degree of water saturation over the unsaturated soil zone. Results are shown for two radiative forcing (RCP) scenarios (red and pink lines for RCP 2.6, blue and green lines for RCP 8.5), and for the two study periods (red and blue lines for 2006-2025, pink and green lines for 2080-2099). The solid lines represent the ensemble mean model result and the dashed lines represent 1 standard deviation around the mean of the corresponding result derived from individual models. The relative degree of soil water saturation (with value 1 corresponding to full saturation) represents the unsaturated soil water content normalized by the saturated soil water content (soil porosity). The month numbering is: January as month 1 through to December as month 12.

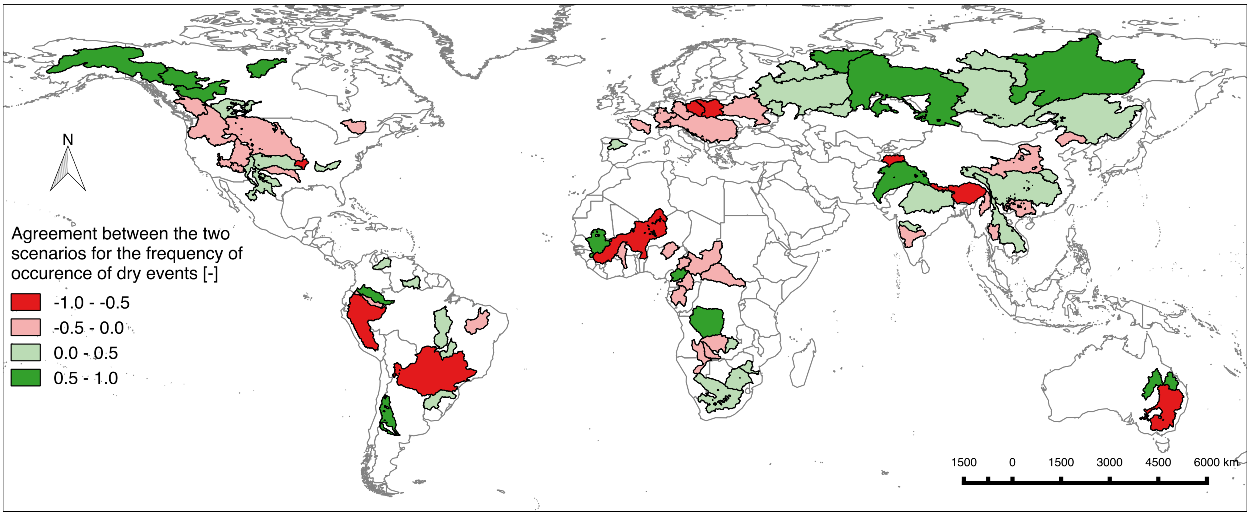

(a)

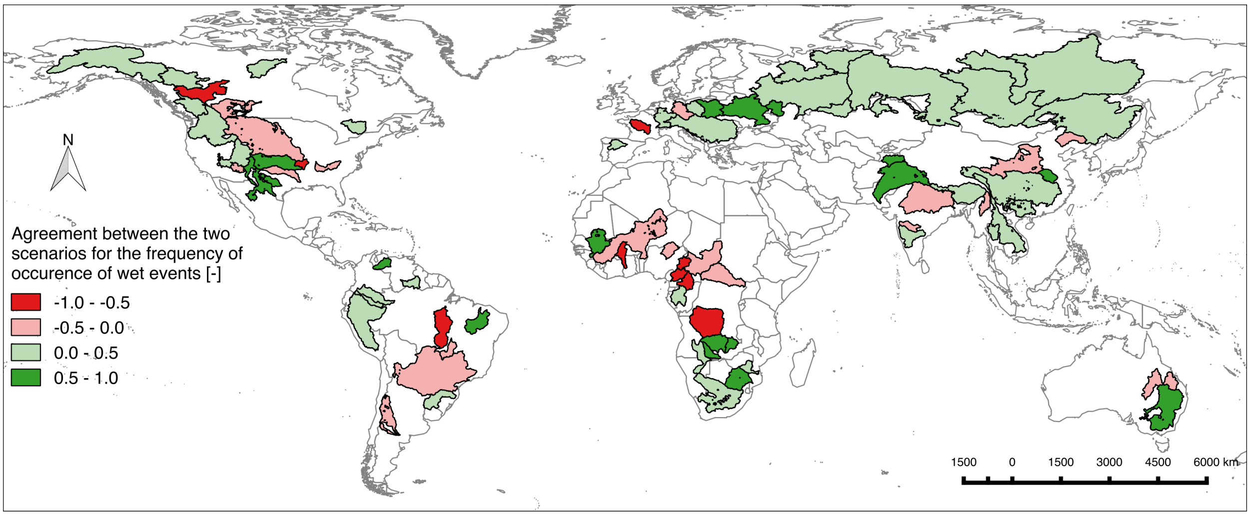

(b)

Figure S5. Map of model result agreement (as defined in SM section S2) between the two radiative forcing scenarios RCP 2.6 and RCP 8.5, regarding the change in occurrence frequency of dry (panel a) and wet (panel b) soil moisture events.

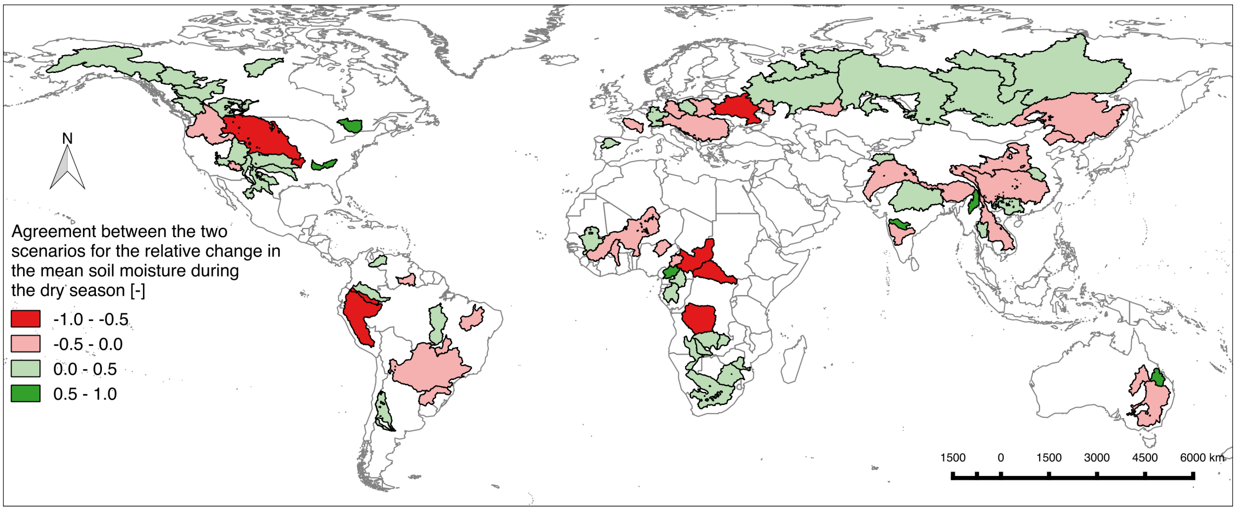

(a)

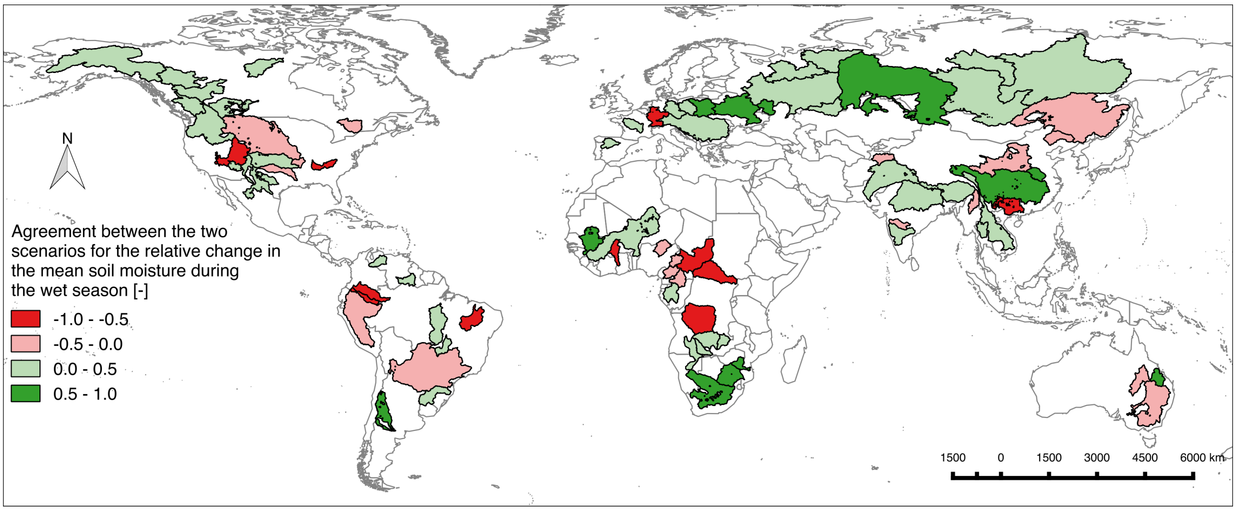

(b)

Figure S6. Map of model result agreement (as defined in SM section S2) between the two radiative forcing scenarios RCP 2.6 and RCP 8.5, regarding the change in mean seasonal soil water content during the dry (panel a) and the wet (panel b) season.

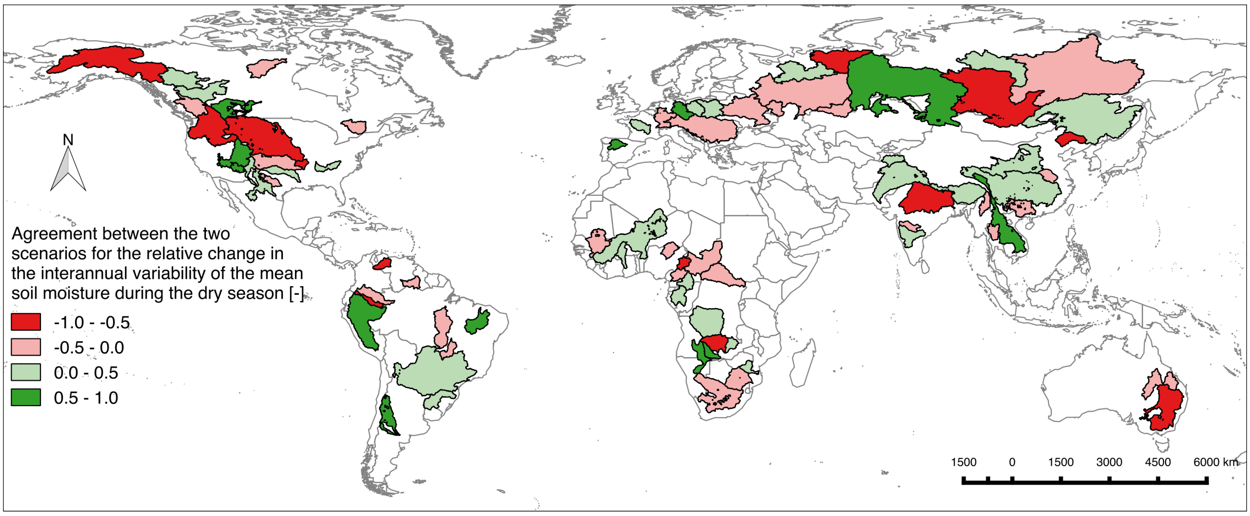

(a)

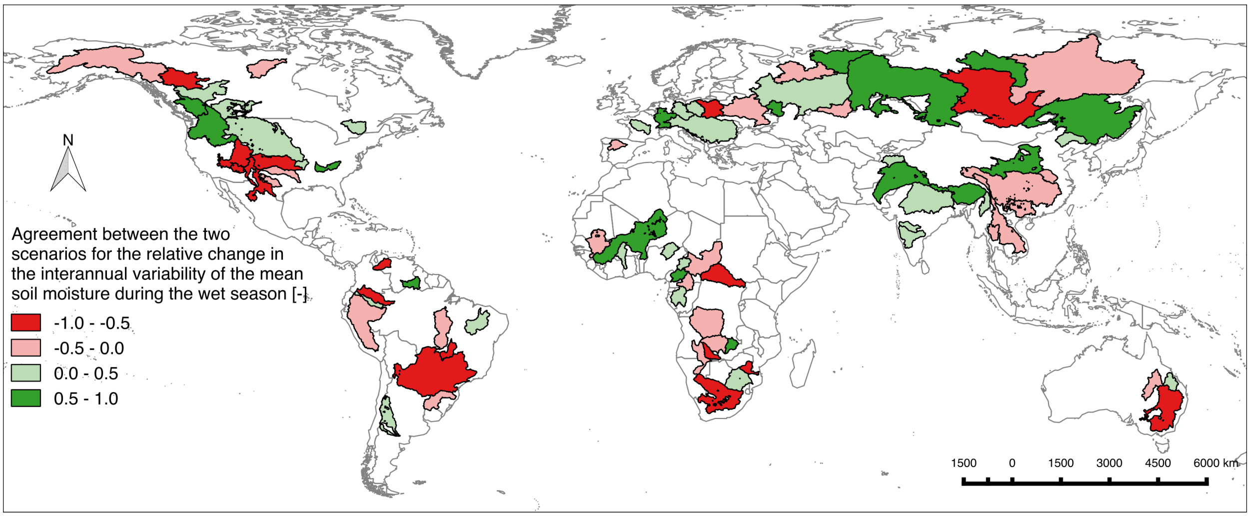

(b)

Figure S7. Map of model result agreement (as defined in SM section S2) between the two radiative forcing scenarios RCP 2.6 and RCP 8.5, regarding the change in inter-annual variability of seasonal soil moisture during the dry (panel a) and the wet (panel b) season.